Title

Whole knee joint T1 values measured in vivo at 3T by combined 3D ultrashort echo time cones actual flip angle and variable flip angle methods

Journal

Magnetic Resonance in Medicine, 81(3)

ISSN

0740-3194

Authors

Ma, Ya-Jun
Zhao, Wei
Wan, Lidi
et al.

Publication Date

2019-03-01

DOI

10.1002/mrm.27510

Peer reviewed

Received: 25 April 2018 | Revised: 6 July 2018 | Accepted: 7 August 2018

DOI: 10.1002/mrm.27510

FULL PAPER

Magnetic Resonance in Medicine

Whole knee joint T_1 values measured in vivo at 3T by combined 3D ultrashort echo time cones actual flip angle and variable flip angle methods

Ya-Jun Ma[1] | **Wei Zhao**[1] | **Lidi Wan**[1] | **Tan Guo**[1] | **Adam Searleman**[1] | **Hyungseok Jang**[1] | **Eric Y. Chang**[1,2] | **Jiang Du**[1]

[1]Department of Radiology, University of California, San Diego, California

[2]Radiology Service, VA San Diego Healthcare System, San Diego, California

Correspondence
Jiang Du, University of California, San Diego, Department of Radiology, 200 West Arbor Drive, San Diego, CA 92103-8226.
Email: jiangdu@ucsd.edu

Funding information
NIH, Grant/Award Numbers: 1R01 AR062581, 1R01 AR068987, and T32EB005970; Veterans Affairs, Grant/Award Numbers: 1I01CX001388 and I01RX002604; GE Healthcare.

Purpose: To measure T_1 relaxations for the major tissues in whole knee joints on a clinical 3T scanner.

Methods: The 3D UTE-Cones actual flip angle imaging (AFI) method was used to map the transmission radiofrequency field (B_1) in both short and long T_2 tissues, which was then used to correct the 3D UTE-Cones variable flip angle (VFA) fitting to generate accurate T_1 maps. Numerical simulation was carried out to investigate the accuracy of T_1 measurement for a range of T_2 values, excitation pulse durations, and B_1 errors. Then, the 3D UTE-Cones AFI-VFA method was applied to healthy volunteers ($N = 16$) to quantify the T_1 of knee tissues including cartilage, meniscus, quadriceps tendon, patellar tendon, anterior cruciate ligament (ACL), posterior cruciate ligament (PCL), marrow, and muscles at 3T.

Results: Numerical simulation showed that the 3D UTE-Cones AFI-VFA technique can provide accurate T_1 measurements (error <1%) when the tissue T_2 is longer than 1 ms and a 150 μs excitation RF pulse is used and therefore is suitable for most knee joint tissues. The proposed 3D UTE-Cones AFI-VFA method showed an average T_1 of 1098 ± 67 ms for cartilage, 833 ± 47 ms for meniscus, 800 ± 66 ms for quadriceps tendon, 656 ± 43 ms for patellar tendon, 873 ± 38 ms for ACL, 832 ± 49 ms for PCL, 379 ± 18 ms for marrow, and 1393 ± 46 ms for muscles.

Conclusion: The 3D UTE-Cones AFI-VFA method allows volumetric T_1 measurement of the major tissues in whole knee joints on a clinical 3T scanner.

KEYWORDS
actual flip angle imaging, knee joint, ultrashort echo time, variable flip angle

1 | INTRODUCTION

Human knee joints are composed of many soft tissues including articular cartilage, menisci, ligaments, tendons, and muscles, all of which are important to the health of the joint.[1-3] Accurate T_1 measurements of the major knee joint tissues can be used for optimization of signal intensity and image contrast.[4] Additionally, T_1 relaxation is a fundamental property of a tissue and may be directly useful as a biomarker of disease or degeneration[5,6] or used to measure other quantitative MRI biomarkers, such as the macromolecular proton fraction from magnetization transfer

modeling or low frequency exchange information from $T_{1\rho}$ imaging.[7-9]

Many T_1 measurement techniques have been proposed including inversion recovery (IR) and saturation recovery (SR) methods, as well as spoiled gradient recalled echo (SPGR)-based variable flip angle (VFA) and variable repetition time (VTR) methods.[10-13] However, conventional MRI pulse sequences (such as SPGR and fast spin echo sequences) are of limited value for imaging deep radial and calcified cartilage, menisci, ligaments, bone, and tendons because these tissues typically have T_2 values ranging from sub-milliseconds to several milliseconds and therefore provide little or no detectable signal.[14-16] In contrast, all of the major knee joint components, including both short and long T_2 tissues, can be imaged using ultrashort echo time (UTE) sequences with TEs <100 μs.[6,14-16] Therefore, combining T_1 measurement techniques with UTE acquisitions has the potential for simultaneous T_1 mapping of the whole knee joint.

However, the IR-based UTE (IR-UTE) method is inaccurate for T_1 measurement of short T_2 tissues because the required inversion pulse is too long (typically on the order of several milliseconds) on currently available clinical scanners to provide complete inversion of the short T_2 magnetization.[17] The SR-based UTE (SR-UTE) method provides more accurate T_1 measurements for short T_2 tissues[13] but would require long scan times for volumetric T_1 mapping. UTE-based VFA or VTR methods can provide volumetric T_1 mapping,[17-22] but they suffer from high sensitivity to B_1 inhomogeneity.[23-26] Obtaining an accurate B_1 map is crucial with VFA and VTR T_1 measurement approaches. Actual flip angle imaging (AFI) is a fast 3D B_1 mapping technique that has been successfully used for correction of VFA- and VTR-based T_1 measurements.[23,25]

UTE-AFI has been recently developed to map flip angles for both short and long T_2 tissues.[22,26] However, with conventional peak power limitations on the RF amplifiers of clinical scanners, the RF pulse duration must be increased to produce the large flip angle excitation (>40°) required for AFI. This longer RF pulse has reduced excitation efficiency (i.e., T_2 relaxation during the RF pulse) for short T_2 tissues, resulting in noticeable errors in the derived B_1 map when the tissue T_2 value is <0.5 ms.[22] T_2 relaxation during the RF pulse results in smaller actual flip angles for short and/or ultrashort T_2 components than the nominal flip angle.

Previously, we have proposed using a UTE AFI-VTR method for accurate T_1 mapping of both short and long T_2 tissues of the knee.[22] The effects of variable excitation efficiency were overcome by using an identical excitation pulse for the UTE-AFI and UTE-VTR sequences.[22] However, UTE AFI-VTR would require a long scan time for 3D high resolution knee imaging, making it unacceptable for clinical use.[22] Because all major knee tissues other than bone have a T_2 value longer than 1 ms,[11,27-33] the B_1 map generated by the UTE-AFI method can still be used for B_1 correction of the faster VFA-based T_1 measurement for these tissues. Therefore, the UTE AFI-VFA method would be expected to provide accurate T_1 measurements of the soft tissues of the whole knee joint with much less scan time than the UTE AFI-VTR method.

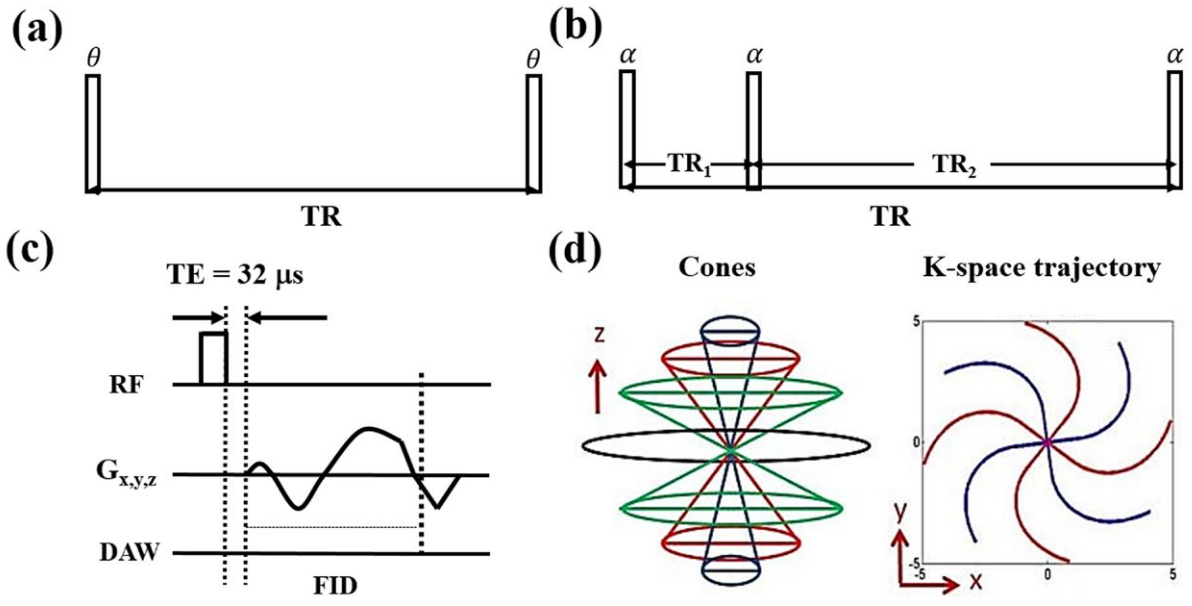

FIGURE 1 The 3D UTE-Cones sequence with a single TR is used for T_1 measurement with the variable flip angle (VFA) method (A). The 3D UTE-Cones actual flip angle imaging (AFI) sequence employs a pair of interleaved TRs for accurate B_1 mapping (B), which together with the VFA method provides accurate T_1 measurements. In these 2 UTE-Cones sequences, a short rectangular pulse is used for signal excitation followed by 3D spiral sampling with a very short TE of 32 μs (C). The spiral trajectories are arranged with conical view ordering (D)

In this study, numerical simulations were carried out to investigate the T_1 measurement accuracy of the UTE AFI-VFA method for the knee joint tissues with a variety of T_2 values on a clinical scanner. Then, we applied the 3D UTE-Cones AFI-VFA method for in vivo whole knee imaging to measure T_1 values of cartilage, meniscus, quadriceps tendon, patellar tendon, anterior cruciate ligament (ACL), posterior cruciate ligament (PCL), marrow, and muscles at 3T.

2 | THEORY

Features of the 3D UTE-Cones pulse sequence with a single TR (Figure 1A) have been described before.[34-36] A series of 3D UTE-Cones acquisitions with variable flip angles are used for T_1 measurement. UTE-AFI can be achieved with the 3D dual TR UTE-Cones sequence (Figure 1B).[22] Both the UTE-Cones AFI and the UTE-Cones VFA sequences use a short rectangular pulse (e.g., RF duration τ = 150 μs) for non-selective signal excitation (Figure 1C) followed by spiral trajectory data acquisition with conical view ordering (Figure 1D).

The generalized signal expressions of S_1 and S_2 for TR_1 and TR_2 of the AFI sequence (Figure 1Bb) for both short and long T_2 tissues are expressed as follows[22]:

$$S_1 = M_0 f_{xy}\left(\alpha,\tau,T_2\right)\frac{1-E_2+\left(1-E_1\right)E_2 f_z\left(\alpha,\tau,T_2\right)}{1-E_1E_2f_z^2\left(\alpha,\tau,T_2\right)} \quad (1)$$

$$S_2 = M_0 f_{xy}\left(\alpha,\tau,T_2\right)\frac{1-E_1+\left(1-E_2\right)E_1 f_z\left(\alpha,\tau,T_2\right)}{1-E_1E_2f_z^2\left(\alpha,\tau,T_2\right)}, \quad (2)$$

with $E_1 = \exp(-TR_1/T_1)$ and $E_2 = \exp(-TR_2/T_1)$.

M_0 is the equilibrium magnetization. $f_{xy}\left(\alpha,\tau,T_2\right)$ and $f_z\left(\alpha,\tau,T_2\right)$ are the respective transverse and longitudinal magnetization mapping functions, which are described as follows[22,37]:

$$f_{xy}\left(\alpha,\tau,T_2\right) = e^{-\frac{\tau}{2T_2}}\alpha\,\mathrm{sinc}\left(\sqrt{\alpha^2-\left(\frac{\tau}{2T_2}\right)^2}\right), \quad (3)$$

$$f_z\left(\alpha,\tau,T_2\right) = e^{-\frac{\tau}{2T_2}}\left(\cos\left(\sqrt{\alpha^2-\left(\frac{\tau}{2T_2}\right)^2}\right)+\frac{\tau}{2T_2}\mathrm{sinc}\left(\sqrt{\alpha^2-\left(\frac{\tau}{2T_2}\right)^2}\right)\right), \quad (4)$$

α is the nominal flip angle and τ is the duration of the rectangular excitation pulse.

With TR_1 and TR_2 that are short relative to T_1, the signal ratio r of S_1 and S_2 can be simplified using a first-order approximation for the exponential terms such that[23]:

$$r = S_2/S_1 \approx \frac{1+nf_z\left(\alpha,\tau,T_2\right)}{n+f_z\left(\alpha,\tau,T_2\right)}, \quad (5)$$

where $n = TR_2/TR_1$. The ratio r can then be used as a T_1-independent measure of $f_z\left(\alpha,\tau,T_2\right)$:

$$f_z\left(\alpha,\tau,T_2\right) \approx \frac{rn-1}{n-r}. \quad (6)$$

For a tissue with $T_2 >> \tau$, $f_{xy}\left(\alpha,\tau,T_2\right)$ and $f_z\left(\alpha,\tau,T_2\right)$ simplify to sin(α) and cos(α), respectively.

Therefore, the actual flip angle α can be accurately estimated with the following equation[22,23]:

$$\alpha \approx \arccos\left(\frac{rn-1}{n-r}\right). \quad (7)$$

The B_1 scaling factor (B_{1s}) is obtained by dividing the measured α by the nominal flip angle α_{nom}:

$$B_{1s} = \alpha/\alpha_{nom}. \quad (8)$$

B_{1s} is used to quantify the RF inhomogeneity, with B_{1s} = 1 corresponding to an unaltered RF field.

The signal equation of VFA-based T_1 measurement with B_1 correction is expressed as follows[38]:

$$S_{spgr} = M_0 sin\left(B_{1s}\theta\right)\frac{1-E_s}{1-E_s\cos\left(B_{1s}\theta\right)}, \quad (9)$$

with $E_s = \exp\left(-TR_s/T_1\right)$.

θ is the nominal flip angle and TR_s is the repetition time of the UTE-Cones sequence.

For tissues with T_2 values comparable to the RF duration τ, the excitation efficiency of the RF pulse decreases with T_2. The high dependency on tissue T_2 in $f_z\left(\alpha,\tau,T_2\right)$ means that Equation (7) is no longer accurate for the calculation of α, resulting in inaccurate B_{1s} estimates.[22] This can result in estimation errors for VFA-based T_1 measurements because the method is sensitive to B_1 errors.

To investigate the accuracy of VFA T_1 measurement with AFI B_1 correction (UTE AFI-VFA) for tissues with a variety of T_2 values on a clinical scanner, numerical simulations were carried out as described below.

3 | METHODS

The 3D UTE-Cones and 3D UTE-Cones AFI sequences (Figure 1) were implemented on a 3T MR750 scanner (GE Healthcare Technologies, Milwaukee, WI). An 8-channel transmit–receive knee coil was used for both RF

transmission and signal reception. Unique k-space trajectories were used in the UTE-Cones sequences that sampled data along evenly spaced twisted paths in the form of multiple cones.[29-31] Data sampling began from the center of k-space and continued outward. It began as soon as practical after the RF excitation with a minimal nominal delay time of 32 μs. Both RF and gradient spoiling were used to crush the remaining transverse magnetizations. In VFA UTE-Cones, the area of the gradient crushers was 180 mT × ms/m and the RF phase increment was 169°. In UTE-Cones AFI, the areas of gradient crushers in TR_1 and TR_2 were 180 and 900 mT × ms/m, respectively, and the RF phase increment was 39°C.[22] The UTE-Cones sequence allowed anisotropic resolution (e.g., higher in-plane resolution and thicker slices) to provide an improved SNR and a reduced scan time relative to isotropic imaging.[30,31]

3.1 | Simulation

Numerical simulation was performed to investigate the accuracy of the proposed UTE AFI-VFA T_1 measurement for relatively short T_2 tissues. The UTE AFI-VFA technique is expected to accurately measure T_1 for long T_2 tissues. Simulated rectangular RF pulses used for signal excitation in both the 3D UTE AFI and VFA sequences had identical durations and ranged from 0.1 to 300 μs. T_2 values of simulated tissues ranged from 0 to 5 ms. The B_1 scaling factors and the ratio between f_{xy} and $\sin(B_{1s}\theta)$ measured with different nominal flip angles (range from 0° to 90°) for short T_2s were also investigated with a pulse duration of 150 μs. This ratio was calculated to investigate whether the obtained B_{1s} could correct the transverse part of the excitation. The T_1 measurement accuracy with the VFA method depends on the accurate correction of both transverse and longitudinal magnetizations after excitation. The T_1 value was set to a constant of 800 ms and M_0 was set to 1. The sequence parameters for UTE AFI and VFA sequences were adjusted as follows: (1) UTE-AFI: TR_1/TR_2 = 20/100 ms and flip angle = 45°; and (2) UTE-VFA: TR = 20 ms, and flip angle = 5°, 10°, 20°, and 30°. B_1 scaling factors and T_1 values with and without B_1 correction were calculated for 3 nominal B_1 scaling factors (B_{1n}): 0.8, 1, and 1.2.

3.2 | *In vivo study*

In vivo whole knee imaging was carried out on 16 healthy volunteers (aged 20–49 y, mean age 34 y; 7 males, 9 females). Informed consent was obtained from all subjects in accordance with guidelines of the institutional review board. The 3D UTE-Cones AFI and VFA sequences were used to scan these knee joints using the same FOV of 15×15×10.8 cm^3 and receiver bandwidth of 166 kHz. Other sequence parameters were: (1) 3D UTE-Cones AFI: TR_1/TR_2 = 20/100 ms, flip angle = 45°, acquisition matrices of 128 × 128×18, readout duration = 924 μs and a total scan time of 4 min 57 sec; 2) 3D VFA UTE-Cones: TR = 20 ms, flip angle = 5°, 10°, 20°, and 30°, acquisition matrices of 256 × 256 × 36, undersampling factor of 0.9, readout duration = 1644 μs and a total scan time of 9 min 28 s.

3.3 | Data analysis

Before T_1 calculation, motion registration was performed for all data sets using the Elastix open source software.[39] Rigid registration was carried out first to correct for tissue translations and rotations, and then non-rigid registration was applied for further fine adjustment (such as scaling and shearing), which is particularly important for soft tissues. The Levenberg-Marquardt algorithm was used to solve the nonlinear fitting of Equation (9) for VFA T_1 measurement. The analysis algorithms written in MATLAB (The MathWorks, Natick, MA) were applied to the DICOM images obtained from the 3D UTE-Cones AFI and VFA UTE-Cones protocols described above. Both T_1 values and fitting errors were calculated. Manually drawn ROIs for the 16 in vivo knees were used to measure the mean and SD T_1 values of various tissues including the articular cartilage, meniscus, quadriceps tendon, patellar tendon, ACL, PCL, marrow, and muscles.

4 | RESULTS

The simulation results with variable pulse durations for a range of T_2s are shown in Figure 2. The top 2 rows show the theoretical longitudinal (M_z or $f_z(\alpha,\tau,T_2)$) and transverse (M_{xy} or $f_{xy}(\alpha,\tau,T_2)$) magnetizations calculated by Equations (3) and (4). Longer RF pulses were shown to be less effective than shorter ones in generating M_{xy} for shorter T_2 tissues. M_z and M_{xy} approached $\cos(\alpha)$ and $\sin(\alpha)$, respectively, as T_2 increased. The third row in Figure 2 shows the estimated B_1 scaling factors B_{1s} computed using the AFI method with Equations (7) and (8). As expected, the measured B_{1s} were more accurate when using shorter RF pulses and when imaging longer T_2 species. Otherwise, the estimated B_{1s} were smaller than the nominal values.

The bottom 2 rows show the simulation results of T_1 measurements using the VFA method without and with B_1 correction. The B_1-uncorrected T_1 values show significant estimation errors and increased with larger values of the nominal B_1 scaling factor B_{1n}. Overall, the T_1 values generated by the B_1-corrected VFA method were much more accurate than the T_1 values measured by the B_1-uncorrected VFA method. However, T_1 estimation errors still existed in the B_1-corrected T_1 values when T_2 values were shorter than 0.5 ms, and the errors became larger with increased B_{1n}. All 3 of the B_1-corrected T_1 maps were separated into 2 regions by

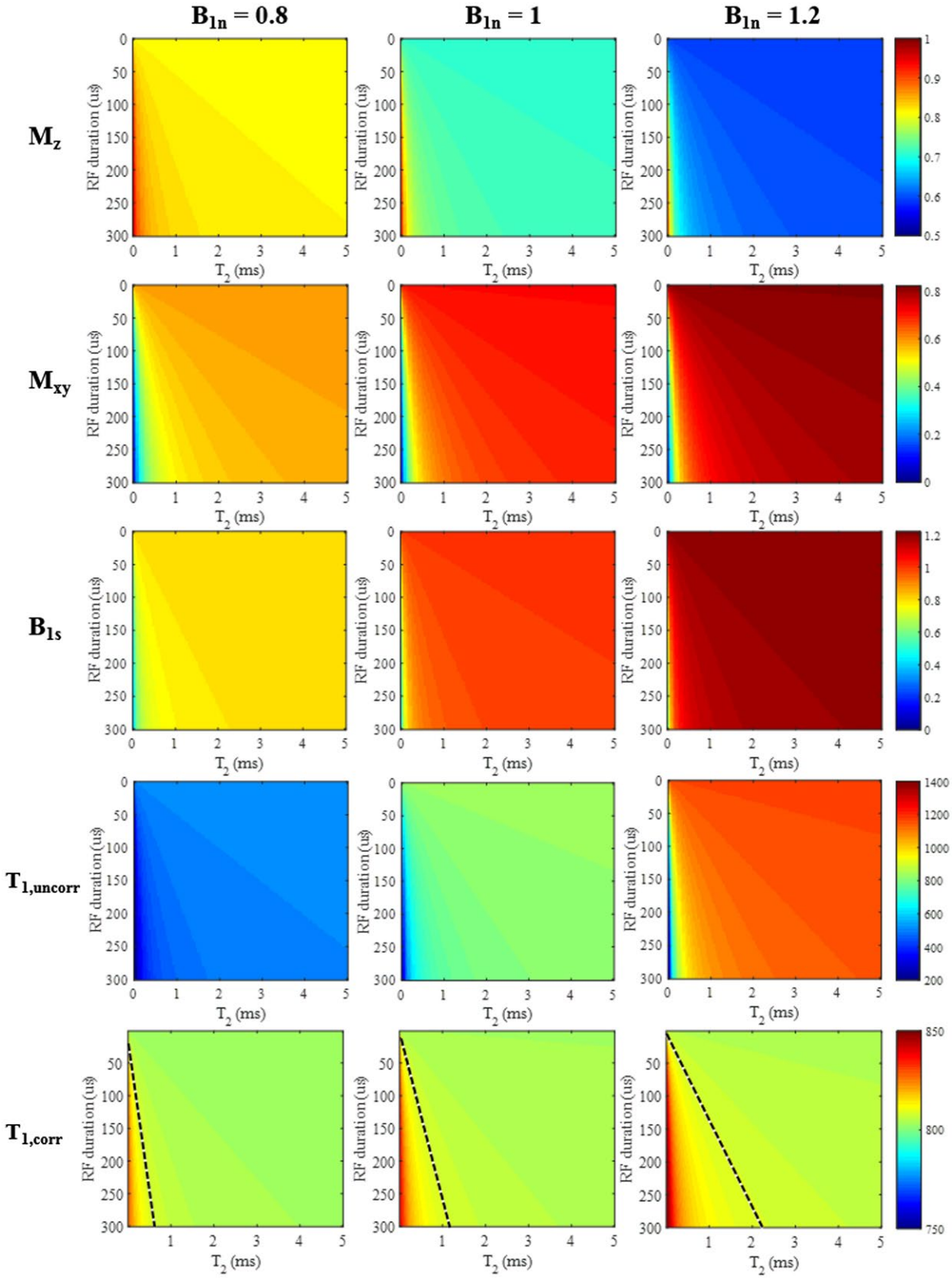

FIGURE 2 Simulation results for different T_2 tissues (T_2 values from 0 to 5 ms) with rectangular RF pulse excitation (durations from 0.1 to 300 μs). The top 2 rows show color maps corresponding to the longitudinal (M_z or $f_z(\alpha,\tau,T_2)$) and transverse (M_{xy} or $f_{xy}(\alpha,\tau,T_2)$) magnetizations calculated from Equations (3) and (4). The third row shows the resulting B_{1s} scaling factors obtained by the AFI method (i.e., Equations (7) and (8). T_1 values (units of ms) generated by the VFA method are shown without (4th row) and with B_{1s} correction (5th row). For the B_1-corrected T_1 results, a dashed black line was drawn such that the region to the left of the line had a T_1 estimation error >1% and the region to the right had an estimation error <1%. The columns represent simulation results with nominal B_1 scaling factors B_{1n} of 0.8, 1, and 1.2, respectively

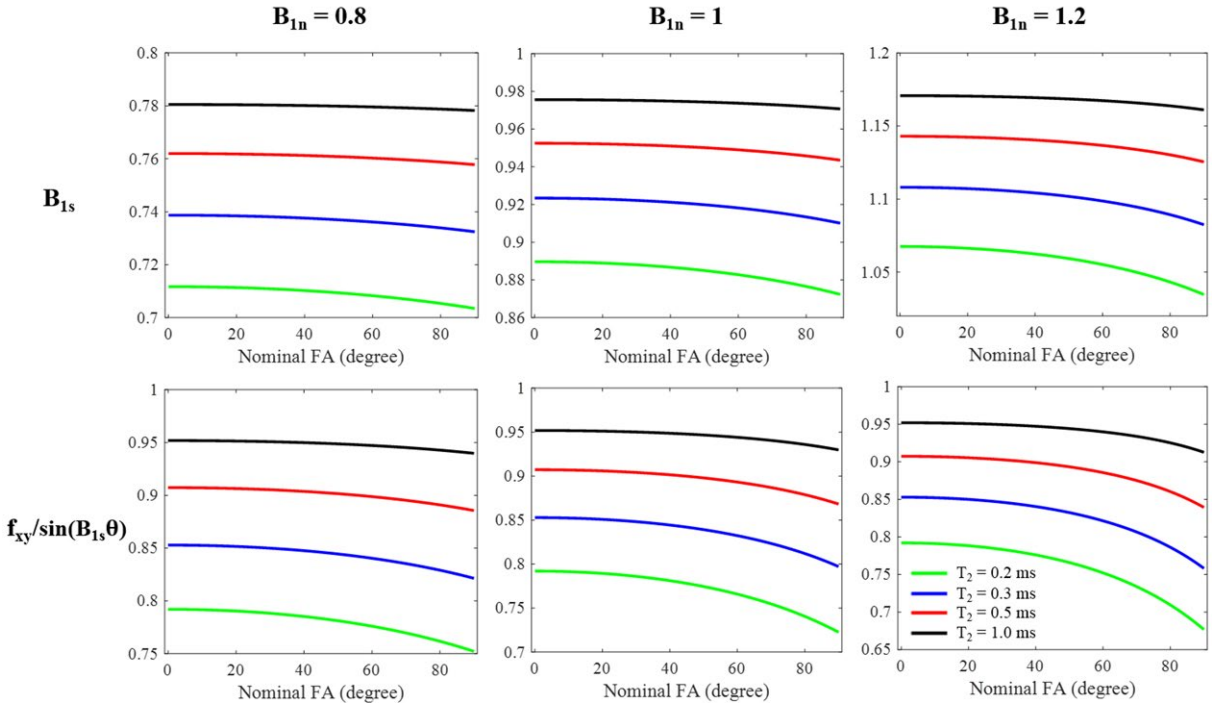

FIGURE 3 Simulation curves for different T_2 tissues (green: 0.2 ms, blue: 0.3 ms, red: 0.5 ms and black: 1 ms) with rectangular RF pulse excitation (nominal FA from 0° to 90°; pulse duration $\tau = 150$ μs). The first row shows the resulting B_1 scaling factors obtained by the AFI method (i.e., Equations (7) and (8). The second row shows the ratio between f_{xy} in Equation (3) and $\sin(B_{1s}\theta)$ in Equation (9). The columns represent simulation results with nominal B_1 scaling factors B_{1n} of 0.8, 1, and 1.2, respectively

dashed black lines: the T_1 estimation errors were higher than 1% in the bottom left portions (triangular shaped area) and the T_1 estimation errors in the other portions were lower than 1%. Therefore, we found that when an excitation pulse with a duration of 150 μs is used for imaging tissues with T_2 values >1 ms, the B_1-corrected T_1 value measured by the AFI-VFA method is accurate with <1% estimation error in the setting of up to 20% B_1 inhomogeneity.

The simulation curves with a range of nominal flip angles for the 4 short T_2s (i.e., 0.2 ms, 0.3 ms, 0.5 ms, and 1 ms) are shown in Figure 3. Both B_1 scaling factors and the ratio between f_{xy} and $\sin(B_{1s}\theta)$ slightly changed with different nominal flip angles. More changes can be found when tissue T_2 is shorter. Therefore, for shorter T_2s, a single correction factor is not good enough to correct the excitation errors in different flip angles for VFA T_1 measurement as shown in the last row of Figure 2. However, both B_{1s} and the ratio almost stay constant for flip angles lower than 50° when T_2 is 1 ms or longer, which demonstrate the accuracy of the proposed AFI-VFA T_1 measurement method for tissues with T_{2s} longer than 1 ms.

Because the articular cartilage, meniscus, quadriceps tendon, patellar tendon, ACL, PCL, marrow, and muscles all have T_2 values longer than 1 ms, the B_1-corrected VFA method with a 150 μs long excitation pulse should be suitable for the measurement of T_1 values of these tissues. The signal intensities of the tissues have been measured before and after registration. There were almost no signal intensity changes because of the motion registration. Figure 4 shows T_1 fitting results for various knee joint tissues of a representative healthy volunteer (age 35, male). All the data show excellent fittings. The proposed 3D UTE-Cones AFI-VFA method showed a T_1 value of 832 ± 18 ms for meniscus, 779 ± 7 ms for quadriceps tendon, 637 ± 16 ms for patellar tendon, 870 ± 13 ms for ACL, 819 ± 17 ms for PCL, 1133 ± 40 ms for cartilage, 386 ± 2 ms for marrow, and 1406 ± 63 ms for muscles of this volunteer.

Figure 5 shows T_1 mapping results of the knee of the same healthy volunteer as above. T_1 maps generated by the proposed 3D UTE-Cones AFI-VFA method are shown in Figures 5D–5F. For comparison, the T_1 maps generated by the 3D UTE-Cones VFA method without B_1 correction are shown in Figures 5G–5I. T_1 estimation errors induced by B_1 inhomogeneity, which are more severe in regions close to the coil boundary, have been corrected by the proposed 3D UTE-Cones AFI-VFA method. Corresponding B_{1s} maps are shown in Figures 5J–5L. As expected, lower B_{1s} values can be found in cortical bone regions because of lower excitation efficiency.

Table 1 summarizes T_1 measurements by the proposed 3D UTE-Cones AFI-VFA method for the principal knee joint tissues of healthy volunteers ($N = 16$). The proposed 3D UTE-Cones AFI-VFA method showed a mean T_1 value and SD of 833 ± 47 ms for meniscus, 800 ± 66 ms for quadriceps tendon, 656 ± 43 ms for patellar tendon, 873 ±

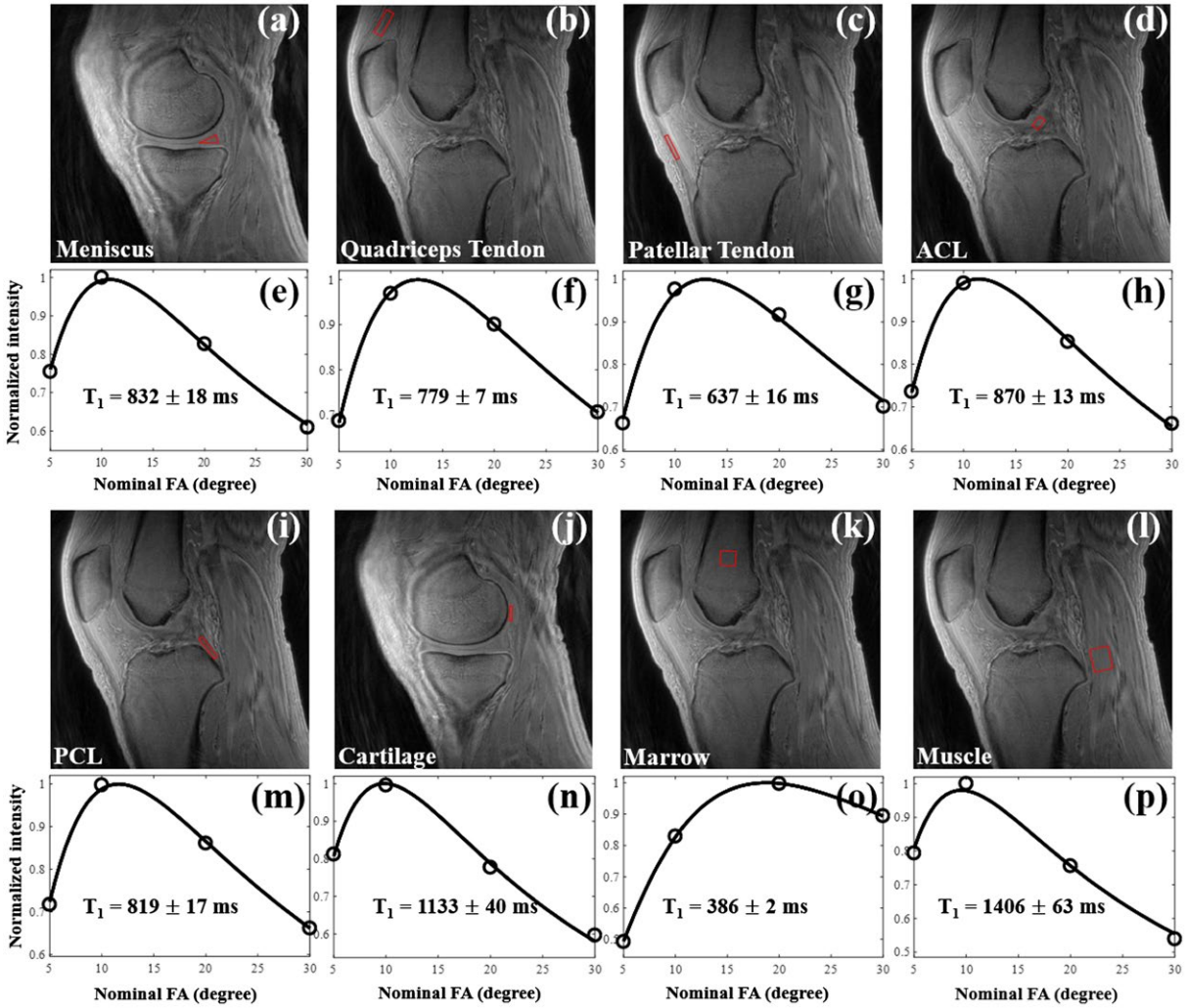

FIGURE 4 T_1 fitting results in knee tissues from a representative healthy volunteer (age 35, male) using the proposed 3D UTE-Cones AFI-VFA method. The measured T_1 values for this volunteer were 832 ± 18 ms for meniscus, 779 ± 7 ms for quadriceps tendon, 637 ± 16 ms for patellar tendon, 870 ± 13 ms for ACL, 819 ± 17 ms for PCL, 1133 ± 40 ms for cartilage, 386 ± 2 ms for marrow, and 1406 ± 63 ms for muscles

38 ms for ACL, 832 ± 49 ms for PCL, 1098 ± 67 ms for cartilage, 379 ± 18 ms for marrow, and 1393 ± 46 ms for muscles.

5 | DICUSSION

We have demonstrated that the proposed 3D UTE-Cones AFI-VFA method can accurately measure T_1 values for most major tissues of the whole knee joint. Simulation shows that the proposed 3D UTE-Cones AFI-VFA method provides accurate T_1 measurements for tissues with T_2 values longer than 1 ms. Because most knee tissues have T_2s longer than 1 ms (meniscus: 5–8 ms, ligament and tendon: 4–10 ms, cartilage: 27–43 ms, muscle: 32–50 ms, and fat: ~133 ms),[11,27-33] accurate T_1 maps were obtained using the proposed method to provide in vivo knee measurements in 16 healthy volunteers.

Because of the high sensitivity in VFA T_1 measurements to B_1 errors, obtaining an accurate B_1 map is crucial. AFI is a fast 3D B_1 mapping technique that fits very well with VFA-based T_1 corrections. It has been used for volumetric B_1 mapping of brain, body, and musculoskeletal tissues.[23,40,41] UTE-AFI techniques using radial trajectories have been implemented for B_1 mapping of short T_2 tissues on both clinical 3T and 9.4T MRI systems.[20,26] Most recently, we have implemented the 3D UTE-Cones-based AFI sequence on a clinical 3T scanner.[22] 3D UTE-Cones uses a spiral trajectory data acquisition with conical view ordering, which provide the flexibility to stretch each spiral interleave to vastly reduce the total number of interleaves. Therefore, combined with the ability for anisotropic resolution, the 3D UTE-Cones data acquisition is much more efficient than the radial UTE acquisition.[34,35]

As shown in the simulation study and a previous cortical bone study,[22] the VFA T_1 maps did not show much

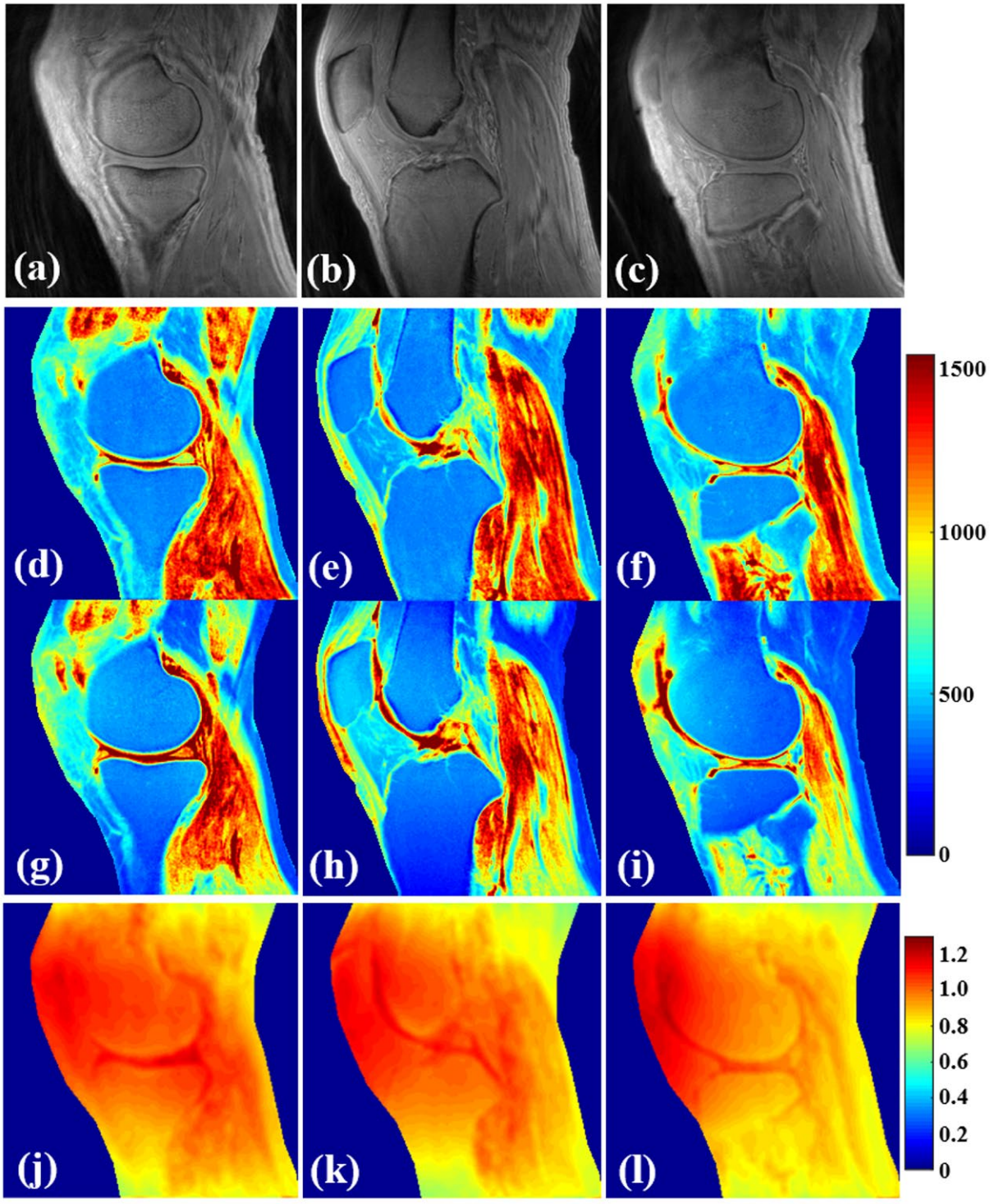

FIGURE 5 Results in knee tissues from a healthy 35-year-old male volunteer (A–L). (A–C) are the selected VFA images with FA = 5°. T_1 mapping using both the proposed 3D UTE-Cones AFI-VFA (D–F) and B_1-uncorrected VFA (G–I) methods are shown. The B_{1s} maps generated by the AFI technique (J–L) are shown. B_1 inhomogeneity induced T_1 estimation errors in the images of (G)–(I) have been corrected by the proposed 3D UTE-Cones AFI-VFA method, especially in regions close to the coil boundary

improvement after B_1 correction for very short T_2 tissues such as cortical bone. However, for tissues with T_2 values longer than 1 ms (much longer than pulse duration of 150 μs), the obtained B_{1s} is almost accurate and AFI-VFA can provide accurate T_1 measurement. The coverage of the simulated nominal B_1 scaling factors B_{1n} from 0.8 to 1.2 should be wide enough for most cases of in vivo knee imaging. Therefore, the proposed 3D UTE-Cones AFI-VFA method was able to

TABLE 1 Mean and SD of T_1 values of knee tissues of 16 healthy volunteers measured by the proposed 3D UTE-Cones AFI-VFA method

Meniscus	Quadriceps tendon	Patellar tendon	ACL
833 ± 47 ms	800 ± 66 ms	656 ± 43 ms	898 ± 63 ms
PCL	Cartilage	Marrow	Muscle
832 ± 49 ms	1098 ± 67 ms	379 ± 18 ms	1393 ± 46 ms

accurately measure T_1 of all the major knee tissues except for bone.

To our best knowledge, this study is the first to report the T_1 values for all the soft tissues in the human knee joint in vivo. Most of previous T_1 measurement studies focused on the articular cartilage, meniscus, and muscle. The T_1 values of the ligaments including quadriceps tendon, patellar tendon, ACL, and PCL have been barely studied because they are not detected by clinical sequences because of their relatively short T_2 values. Our measured T_1 values for cartilage (~1098 ms), muscle (~1393 ms), and marrow (~379 ms) at 3T are comparable with previous 3T studies. For example, Stanisz et al.[11] reported T_1 values of 1156 ms for cartilage and 1412 ms for skeletal muscle; Gold et al.[33] reported T_1 values of 1240 ms for cartilage, 1420 ms for skeletal muscle, and 365 ms for marrow; and Jordan et al.[42] reported T_1 values of 1016 ms for cartilage, 1256 ms for muscle, and 381 ms for marrow. We recently measured in vivo cortical bone T_1 values of ~220 ms using a related 3D UTE-Cones AFI-VTR method.[22]

Magnetization transfer (MT) effects were not considered for both the AFI B_1 scaling factor and VFA T_1 quantification in this study. Because most tissues in our study (e.g., cartilage and menisci) have high macromolecular contents, MT effects can lead to T_1 measurement errors for the AFI-VFA method.[43,44] Further work should consider and correct MT effects for more accurate T_1 measurement. In addition, an interesting finding is that the B_{1s} maps in Figure 5 show contrast between fat and other tissues. This may be a result from the MT effect because fat has negligible MT effect in comparison to other tissues. Another possible explanation for the contrast is the different dielectric properties of fat and other tissues.[45] Secondary B_1 field components can be generated by tissue-specific-induced current densities. Therefore, the higher B_{1s} values observed in cartilage, menisci, and muscle may also result from greater induced current densities, because their conductivity and permittivity values are much greater than those of fat.[46] Previous authors have investigated tissue dielectric properties based on the transmit B_1 maps.[47,48]

There are also several limitations of this study. First, the total data acquisition time is relatively long, in part because of the parameters selected for high accuracy, high image resolution, and broad spatial coverage. A number of strategies can be used to reduce the total scan time, including decreasing the total number of FAs for VFA,[10] using lower resolution for B_1 mapping, and advanced techniques for image reconstruction such as parallel imaging and compressed sensing reconstruction.[49] Second, fat and chemical shift artifacts (that produce ring artifacts in 3D UTE-Cones imaging) may lead to errors in T_1 estimation, necessitating some form of fat–water signal separation to improve accuracy.[50]

6 | CONCLUSION

The 3D UTE-Cones AFI-VFA method provides a robust technique for volumetric T_1 mapping of all the soft tissues in knee joints in vivo with a clinical 3T scanner, including the articular cartilage, meniscus, quadriceps tendon, patellar tendon, ACL, PCL, marrow, and muscles.

ACKNOWLEDGMENTS

The authors acknowledge grant support from NIH (1R01 AR062581, 1R01 AR068987, and T32EB005970), the Veterans Affairs (1I01CX001388 and I01RX002604), and GE Healthcare.

ORCID

Lidi Wan http://orcid.org/0000-0001-6851-4583

REFERENCES

1. Brandt KD, Radin EL, Dieppe PA, Putte L. Yet more evidence that osteoarthritis is not a cartilage disease (Editorial). *Ann Rheum Dis*. 2006;65:1261–1264.
2. Hunter DJ, Zhang YQ, Niu JB, et al. The association of meniscal pathologic changes with cartilage loss in symptomatic knee osteoarthritis. *Arthritis Rheum*. 2006;54:795–801.
3. Tan AL, Toumi H, Benjamin M, et al. Combined high-resolution magnetic resonance imaging and histological examination to explore the role of ligaments and tendons in the phenotypic expression of early hand osteoarthritis. *Ann Rheum Dis*. 2006;65:1267–1272.
4. Zawadzki MB, Gillan GD, Nitz WR. MP-RAGE: a three-dimensional, T1-weighted, gradient-echo sequence–initial experience in the brain. *Radiology*. 1992;182:769–775.

5. Burstein D, Velyvis J, Scott KT, et al. Protocol issues for delayed Gd (DTPA) 2-enhanced MRI (dGEMRIC) for clinical evaluation of articular cartilage. *Magn Reson Med*. 2001;45:36–41.
6. Tiderius CJ, Olsson LE, Leander P, Ekberg O, Dahlberg L. Delayed gadolinium-enhanced MRI of cartilage (dGEMRIC) in early knee osteoarthritis. *Magn Reson Med*. 2003;49:488–492.
7. Ma YJ, Chang EY, Carl M, Du J. Quantitative magnetization transfer ultrashort echo time imaging using a time-efficient 3D multispoke Cones sequence. *Magn Reson Med*. 2018;79:692–700.
8. Ma YJ, Carl M, Shao H, Tadros AS, Chang EY, Du J. Three-dimensional ultrashort echo time cones T1ρ (3D UTE-cones-T1ρ) imaging. *NMR Biomed*. 2017;30:e3709.
9. Ma YJ, Carl M, Searleman A, Lu X, Chang EY, Du J. 3D adiabatic T1ρ prepared ultrashort echo time cones sequence for whole knee imaging. *Magn Reson Med*. 2018;80:1429–1439.
10. Deoni SC, Rutt BK, Peters TM. Rapid combined T1 and T2 mapping using gradient recalled acquisition in the steady state. *Magn Reson Med*. 2003;49:515–526.
11. Stanisz GJ, Odrobina EE, Pun J, et al. T1, T2 relaxation and magnetization transfer in tissue at 3T. *Magn Reson Med*. 2005;54:507–512.
12. Stikov N, Boudreau M, Levesque IR, Tardif CL, Barral JK, Pike GB. On the accuracy of T1 mapping: searching for common ground. *Magn Reson Med*. 2015;73:514–522.
13. Techawiboonwong A, Song HK, Leonard MB, Wehrli FW. Cortial bone water: in vivo quantification with ultrashort echo-time MR imaging. *Radiology*. 2008;248:824–833.
14. Chang EY, Du J, Bae WC, Chung CB. Qualitative and quantitative ultrashort echo time imaging of musculoskeletal tissues. *Semin Musculoskelet Radiol*. 2015;19:375–386.
15. Du J, Carl M, Diaz E, Takahashi A, et al. Ultrashort TE T1rho (UTE T1rho) imaging of the Achilles tendon and meniscus. *Magn Reson Med*. 2010;64:834–842.
16. Du J, Carl M, Bae WC, et al. Dual inversion recovery ultrashort echo time (DIR-UTE) imaging and quantification of the zone of calcified cartilage (ZCC). *Osteoarthritis Cartilage*. 2013;21:77–85.
17. Horch RA, Gochberg DF, Nyman JS, Does MD. Clinically compatible MRI strategies for discriminating bound and pore water in cortical bone. *Magn Reson Med*. 2012;68:1774–1784.
18. Chen J, Chang EY, Carl M, et al. Measurement of bound and pore water T1 relaxation times in cortical bone using three-dimensional ultrashort echo time cones sequences. *Magn Reson Med*. 2017;77:2136–45.
19. Du J, Bydder GM. Qualitative and quantitative ultrashort-TE MRI of cortical bone. *NMR Biomed*. 2013;26:489–506.
20. Han M, Larson PEZ, Krug R, Rieke V. Actual flip angle imaging to improve T1 measurement for short T2 tissues. In Proceedings of the 23rd Annual Meeting of ISMRM, Toronto, Canada, 2015, p. 501.
21. Han M, Rieke V, Scott SJ, et al. Quantifying temperature-dependent T1 changes in cortical bone using ultrashort echo-time MRI. *Magn Reson Med*. 2015;74:1548–1555.
22. Ma YJ, Lu X, Carl M, et al. Accurate T1 mapping of short T2 tissues using a three-dimensional ultrashort echo time cones actual flip angle imaging variable repetition time (3D UTE-Cones AFI-VTR) method. *Magn Reson Med*. 2018;80:598–608.
23. Yarnykh VL. Actual flip-angle imaging in the pulsed steady state: a method for rapid three-dimensional mapping of the transmitted radiofrequency field. *Magn Reson Med*. 2007;57:192–200.
24. Deoni SC. High-resolution T1 mapping of the brain at 3T with driven equilibrium single pulse observation of T1 with high-speed incorporation of RF field inhomogeneities (DESPOT1-HIFI). *J Magn Reson Imaging*. 2007;26:1106–1111.
25. Yarnykh VL. Optimal radiofrequency and gradient spoiling for improved accuracy of T1 and B1 measurements using fast steadystate techniques. *Magn Reson Med*. 2010;63:1610–1626.
26. Kobayashi N, Garwood M. B1 mapping of short T2* spins using a 3D radial gradient echo sequence. *Magn Reson Med*. 2014;71:1689–1699.
27. Robson MD, Gatehouse PD, Bydder M, Bydder GM. Magnetic resonance: an introduction to ultrashort TE (UTE) imaging. *J Comput Assist Tomog*. 2003;27:825–846.
28. Wilson KJ, Surowiec RK, Ho CP, et al. Quantifiable imaging biomarkers for evaluation of the posterior cruciate ligament using 3-T magnetic resonance imaging: a feasibility study. *Orthop J Sports Med*. 2016;4:2325967116639044.
29. Liu F, Kijowski R. Assessment of different fitting methods for in-vivo bi-component T2* analysis of human patellar tendon in magnetic resonance imaging. *Muscles Ligaments Tendons J*. 2017;7:163–172.
30. Williams A, Qian Y, Golla S, Chu CR. UTE-T2∗ mapping detects sub-clinical meniscus injury after anterior cruciate ligament tear. *Osteoarthritis Cartilage*. 2012;20:486–494.
31. Du J, Diaz E, Carl M, Bae W, Chung CB, Bydder GM. Ultrashort echo time imaging with bicomponent analysis. *Magn Reson Med*. 2012;67:645–649.
32. Ma YJ, Chang EY, Bydder GM, Du J. Can ultrashort-TE (UTE) MRI sequences on a 3-T clinical scanner detect signal directly from collagen protons: freeze–dry and D2O exchange studies of cortical bone and Achilles tendon specimens. *NMR Biomed*. 2016;29:912–917.
33. Gold GE, Han E, Stainsby J, Wright GA, Brittain J, Beaulieu C. Musculoskeletal MRI at 3.0T: relaxation times and image contrast. *AJR Am J Roentgenol*. 2004;183:343–350.
34. Gurney PT, Hargreaves BA, Nishimura DG. Design and analysis of a practical 3D cones trajectory. *Magn Reson Med*. 2006;55:575–582.
35. Carl M, Bydder GM, Du J. UTE imaging with simultaneous water and fat signal suppression using a time-efficient multispoke inversion recovery pulse sequence. *Magn Reson Med*. 2016;76:577–582.
36. Ma YJ, Zhu Y, Lu X, Carl M, Chang EY, Du J. Short T2 imaging using a 3D double adiabatic inversion recovery prepared ultrashort echo time cones (3D DIR-UTE-Cones) sequence. *Magn Reson Med*. 2018;79:2555–2563.
37. Sussman MS, Pauly JM, Wright GA. Design of practical T2-selective RF excitation (TELEX) pulses. *Magn Reson Med*. 1998;40:890–899.
38. Hurley SA, Yarnykh VL, Johnson KM, Field AS, Alexander AL, Samsonov AA. Simultaneous variable flip angle–actual flip angle imaging method for improved accuracy and precision of three-dimensional T1 and B1 measurements. *Magn Reson Med*. 2012;68:54–64.

39. Klein S, Staring M, Murphy K, Viergever MA, Pluim JP. Elastix: a toolbox for intensity-based medical image registration. *IEEE transactions on medical imaging*. 2010;29:196–205.
40. Sinclair CD, Samson RS, Thomas DL, Weiskopf N, Lutti A, Thornton JS, Golay X. Quantitative magnetization transfer in in vivo healthy human skeletal muscle at 3 T. *Magn Reson Med*. 2010;64:1739–1748.
41. Baudrexel S, Nürnberger L, Rüb U, et al. Quantitative mapping of T1 and T2* discloses nigral and brainstem pathology in early Parkinson's disease. *Neuroimage*. 2010;51:512–520.
42. Jordan CD, Saranathan M, Bangerter NK, Hargreaves BA, Gold GE. Musculoskeletal MRI at 3.0T and 7.0T: a comparison of relaxation times and image contrast. *Eur J Radiol*. 2013;82:734:739.
43. Mossahebi P, Yarnykh VL, Samsonov A. Analysis and correction of biases in cross-relaxation MRI due to biexponential longitudinal relaxation. *Magn Reson Med*. 2014;71:830–838.
44. Bieri O, Scheffler K. On the origin of apparent low tissue signals in balanced SSFP. *Magn Reson Med*. 2006;56:1067–1074.
45. Brink WM, Börnert P, Nehrke K, Webb AG. Ventricular B1+ perturbation at 7 T–real effect or measurement artifact? *NMR Biomed*. 2014;27:617–620.
46. Gabriel S, Lau RW, Gabriel C. The dielectric properties of biological tissues: III. Parametric models for the dielectric spectrum of tissues. *Phys Med Biol*. 1996;41:2271.
47. Voigt T, Katscher U, Doessel O. Quantitative conductivity and permittivity imaging of the human brain using electric properties tomography. *Magn Reson Med*. 2011;66:456–466.
48. Bulumulla SB, Lee SK, Yeo DT. Conductivity and permittivity imaging at 3.0. *T. Concepts Magn Reson Part B Magn Reson Eng*. 2012;41:13–21.
49. Lustig M, Donoho D, Pauly JM. Sparse MRI: the application of compressed sensing for rapid MR imaging. *Magn Reson Med*. 2007;58:1182–1195.
50. Rakow-Penner R, Daniel B, Yu H, Glover AS. Glover GH. Relaxation times of breast tissue at 1.5T and 3T measured using IDEAL. *J Magn Reson Imaging*. 2006;23:87–91.

How to cite this article: Ma Y-J, Zhao W, Wan L, et al. Whole knee joint T_1 values measured in vivo at 3T by combined 3D ultrashort echo time cones actual flip angle and variable flip angle methods. *Magn Reson Med*. 2019;81:1634–1644. https://doi.org/10.1002/mrm.27510